Aluminium alloy cross-sections under uniaxial bending and compression: A numerical study

Aluminium alloy cross-sections under uniaxial bending and compression: A numerical study

Evangelia Georgantzia[1], Michaela Gkantou[1,*], George S. Kamaris[1], Kunal Kansara[1], Khalid Hashim[1,2]
[1]School of Civil Engineering and Built Environment, Liverpool John Moores University, United Kingdom
[2] Faculty of Engineering, University of Babylon, Babylon, Iraq.

E-mail: E.Georgantzia@2019.ljmu.ac.uk

Abstract. The current study numerically investigates the structural behaviour of aluminium alloy square and rectangular hollow cross-sections under compression and uniaxial bending. Material and geometric nonlinear responses were carefully considered within finite element modelling. Geometric imperfections were also included through the execution of an initial eigenvalue buckling analysis. A thorough parametric study was carried out over a range of width-to-thickness ratios used in practice. Different initial loading eccentricities were examined generating various ratios of compressive axial load and bending moment at failure. The relatively new 6082-T6 heat-treated aluminium alloy, which is increasingly employed in structural applications owing to its high strength, was selected for this study. Based on the obtained numerical capacities, the EN 1999-1-1 design interaction curves were assessed providing rather conservative predictions, particularly for the stockiest cross-sections. The simplified Continuous Strength Method was, also, evaluated exhibiting slightly more accurate with less scattering strength provisions.

1. Introduction

Recently aluminium alloy tubular elements have been widely employed in the construction field owing to their advantageous features, such as ease of extrusion, high strength-to-weight ratio and excellent resistance against corrosion. Moreover, hollow cross-sections present efficient structural response against compression, torsional and bending loading. Therefore, they are a suitable choice for structural applications with high demands of strength. European design standards [1] are available for the structural design of aluminium structures, but these were largely based on concepts for steel structures, leading often to inaccurate strength predictions [2]. On this direction, numerous concentric stub column tests with supplementary numerical studies [3-11] have been performed aiming to investigate the local buckling behaviour of square and rectangular hollow section (SHS/RHS) columns subjected to axial compressive loading. The obtained data have been utilised to evaluate the existing design specifications and propose cross-sectional classification criteria in line with the observed response. In real structures the compressive axial loading is often applied eccentrically due to geometrical and constructional imperfections leading to combined bending and compression loading conditions. Hence, focus of this study is the cross-sectional response of SHS/RHSs under combined uniaxial bending and compression, whose research and understanding remain scarce [12].

Aiming to obtain a deeper knowledge on the local buckling behaviour of aluminium tubular cross-sections, this paper investigates numerically the cross-sectional response of RHS and SHS columns formed by 6082-T6 heat-treated aluminium alloy, which is increasingly employed in structural applications owing to its high strength. A refined finite element (FE) model of a stub column was developed in the commercially available package ABAQUS version 6.14 [13]. A parametric study has been conducted considering various parameters, such as cross-sectional aspect ratio (*h/b*) and width-to-thickness ratio (*b/t*) covering the four classes specified in EN 1999-1-1 [1]. A wide range of initial loading eccentricities were also examined generating performance data between pure compression and pure bending states. Finally, the column capacities predicted by the FE models were used to assess the design formulae provided by EN 1999-1-1 [1] and the simplified Continuous Strength Method (CSM).

2. Numerical modelling

2.1. Overview of the study

A numerical study was conducted to examine the cross-sectional response of aluminium alloy tubular stub columns under eccentric compressive loading. The length of both SHS/RHS stub columns was considered as three times larger the cross-sectional height. This allows the geometric imperfections to be adequately developed and prevents global buckling [14]. Two aspect ratios (*h/b*) of 1 (SHS) and 2 (RHS) have been generated considering cross-sectional height of 75 mm and 150 mm. The cross-sectional thickness was determined to consider a wide range of width-to-thickness ratios (*b/t*) covering the four classes specified in EN 1999-1-1 [1]. Thereby, the cross-sectional thicknesses were set equal to 2, 4, 6 and 8 mm in case of the SHSs and 4, 6, 8, 10 and 13 mm in case of the RHSs. The local buckling behaviour of the RHS columns was investigated about both major and minor axes. The initial loading eccentricities (*e*) were determined at 10, 20, 30, 40, 50 and 60 mm generating various ratios of axial compressive loading and bending moment at failure. The states of pure axial compression and pure bending were also studied for the considered cross-sections. In total, 84 FE models were analysed, as summarised in Table 1.

Table 1. List of parametric studies

Total analyses: 84	
1 material	• 6082-T6
3 cross-sections	• 75×75 (SHS) • 75×150 (RHS - uniaxial bending in minor axis & compression) • 150×75 (RHS - uniaxial bending in major axis & compression)
4 cross-sectional thicknesses	• 2, 4, 6, 8 mm (for 75×75 SHS) • 6, 8, 10, 13 mm (for 75×150 RHS) • 4, 6, 8, 10 mm (for 150×75 RHS)
8 loading conditions	• Pure axial compression • Six eccentricities: e= 10, 20, 30, 40, 50, 60 mm • Pure bending

2.2. Modelling assumptions

2.2.1. Element type and discretisation. The general purpose four-noded shell element with reduced integration (S4R) was adopted to model the geometries of the aluminium tubes. This element type is a reasonable choice as it allows for capturing the buckling behaviour of thin-walled structural elements and has already been employed successfully in similar studies [10,15]. Upon the execution of a mesh convergence study, the mesh size was set equal to the wall thickness thus achieving low computational

cost without compromising the accuracy of the results. A typical specimen was discretised in 8000 elements.

2.2.2. Boundary conditions. The applied boundary conditions of a typical FE model are illustrated in figure 1. Reference points (RPs) were created at the geometric centre of the top and bottom end cross-sections to apply the boundary conditions. The degrees of freedom (DOF) between the RPs and the corresponding end surfaces were coupled using rigid body constraints. All translational DOF of both RPs were restrained except the translation at the longitudinal axis at the top loaded RP and the rotation of the relevant axis.

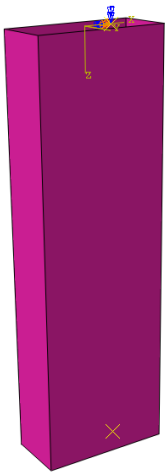

Top support:
Rigid body constraint:
$u_x = u_{rx} = u_y = u_{rz} = 0$ (for major axis bending & compression)
$u_x = u_y = u_{ry} = u_{rz} = 0$ (for minor axis bending & compression)

Bottom support:
Rigid body constraint:
$u_x = u_{rx} = u_y = u_z = u_{rz} = 0$ (for major axis bending & compression)
$u_x = u_y = u_{ry} = u_z = u_{rz} = 0$ (for minor axis bending & compression)

Figure 1. Typical FE model and applied boundary conditions.

Further to eccentric stub columns, the cross-sectional performance in pure bending was investigated considering 4-point bending loading conditions. In this case, the beams were modelled with span-to-height ratio equal to 15 in order to exclude any shear effect. Each loading point was defined at distance of one third of the length from the beam's end. The translational degrees of freedom were restrained expect the longitudinal ones at both ends [16]. For the concentric stub columns, fixed support conditions were considered [11,17].

2.2.3. Material modelling. The constitutive properties reported for 6082-T6 heat-treated aluminium alloy by Georgantzia et al. [18] were adopted in the present study. The rounded stress-strain (σ-ε) behaviour of the examined aluminium alloys was described using the material model proposed by [19]:

$$\varepsilon = \frac{\sigma}{E} + 0.002\left(\frac{\sigma}{\sigma_{0.2}}\right)^n \quad (1)$$

$$n = \frac{ln\,2}{ln\left(\frac{\sigma_{0.2}}{\sigma_{0.1}}\right)} \quad (2)$$

where $\sigma_{0.1}$ and $\sigma_{0.2}$ are the proof strength corresponding to 0.1% and 0.2% strains, respectively, and n is the strain hardening exponent.

A bilinear elastic-plastic behaviour associated with isotropic hardening and von Mises yield criterion was adopted for the aluminium alloys. The Poisson's ratio (v) was set equal to 0.3 as suggested by [1].

Equations (3) and (4) were used to translate the calculated engineering stress strain curves into true stress and true (logarithmic) strain curves so that to simulate the material plasticity.

$$\sigma_{true} = \sigma(1+\varepsilon) \tag{3}$$

$$\varepsilon_{\ln}^{pl} = \ln(1+\varepsilon) - \frac{\sigma_{true}}{E} \tag{4}$$

where σ_{true} and σ are the true and engineering stress, accordingly, and ε and $\varepsilon^{ln}{}_{pl}$ are the engineering and logarithmic plastic strain, accordingly.

2.2.4. Analyses. Thin-walled members are susceptible to buckling which can significantly influence the structural performance and the ultimate load level. Buckling can be triggered by the initial geometric imperfections generated during the manufacturing process and thus they should be considered carefully in the analyses. This can be achieved executing an initial eigenvalue buckling analysis through which the lowest mode shape is obtained and introduced in the subsequent nonlinear analysis. The full range load-axial shortening and load-lateral displacement curves were captured through a non-linear static analysis employing the modified Riks [14] solution method. The axial compressive loading was imposed at the top RP in the form of displacement.

2.3. Validation of the FE model

In absence of literature test results for aluminium alloy stub columns subjected to eccentric compressive loading, experimental data on SHS and RHS steel eccentric stub columns [20] have been used to validate the developed FE models. Applying the modelling assumptions described in section 2.2 along with the geometry and material properties of [20], the reported experiments on stub columns were replicated by FE models. Typical experimental and FE analysis load-lateral displacement curves are depicted in figure 2(a) showing that they match closely in terms of the initial stiffness and overall response. Typical failure modes are also illustrated in figure 2(b) denoting high similarity of the response regarding the local buckling failure modes. Overall, the developed FE models are capable of accurately capturing the cross-sectional response of tubular eccentric stub columns.

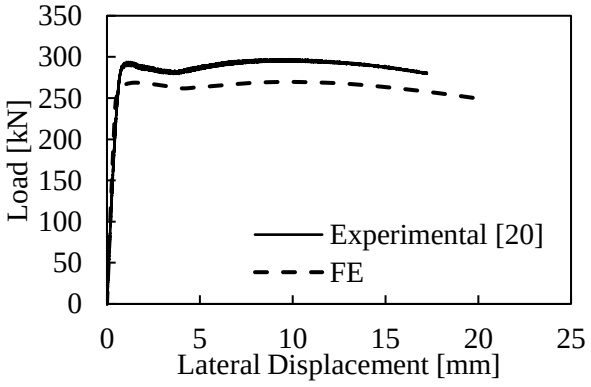

a) S460 SHS 50×50×5 (*e*=10 mm)

b) S690 SHS 90×90×5.6 (e=5 mm)

Figure 2. Comparison of experimental [20] and numerical results.

2.4. Parametric study results

Following the execution of the nonlinear analyses on aluminium alloy eccentric stub columns using the validated FE models, the results were evaluated. The obtained failure modes included material yielding, material yielding combined with inelastic local buckling and elastic local buckling. Figure 3 illustrates typical failure modes of eccentrically loaded stub columns, including the case of SHS under uniaxial bending and compression, an RHS under uniaxial bending in major axis and compression and an RHS

under uniaxial bending in minor axis and compression. The ultimate cross-sectional capacity, $N_{u,FEA}$, axial shortening and the corresponding lateral displacement at the mid-height were captured for each case. The load-axial shortening and load-mid-height lateral displacement curves for some typical cases are illustrated in Figures 4(a) and 4(b). Figure 4(a) depicts the response of a SHS column with increasing eccentricity, while in Figure 4(b) the load-displacement curves for an RHS with fixed *e* but increasing wall thickness is presented.

a) SHS under uniaxial bending and compression

b) RHS under uniaxial bending in major axis and compression

c) RHS under uniaxial bending in minor axis and compression

Figure 3. Typical failure modes of eccentrically loaded stub columns.

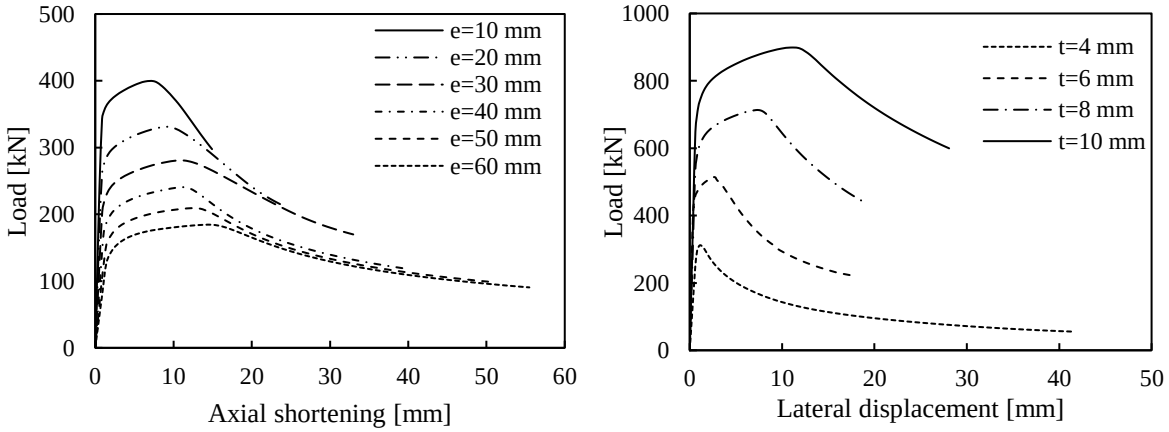

a) SHS, t= 6mm

b) RHS, major axis, e=30 mm

Figure 4. Typical load-axial shortening and load-mid-height lateral displacement curves.

3. Assessment of European Standards

The FE analysis strengths have been utilised for the assessment of the *N-M* interaction curves provided by EN 1999-1-1 [1]. To this end the maximum axial compressive force (N_u) and the maximum bending moment (M_u) accounting for second-order effects were normalised by their corresponding resistances which depend on the cross-sectional class. According to EN 1999-1-1 [1], the aluminium alloy cross-sections are classified in four different classes, according to their susceptibility to local buckling. Classes 1,2 and 3 include the cross-sections in which local buckling occurs after yielding at the plastic range.

Conversely, class 4 cross-sections fail due to local buckling at the elastic range and thereby their is reduced. The resistance of a cross-section under axial compression is determined as follows [1]:

$$N_{Rd} = \begin{cases} A \cdot f_y & \text{for classes 1, 2 \& 3} \\ A_{eff} \cdot f_y & \text{for class 4} \end{cases} \quad (5)$$

where f_y is the yield (proof) strength of the aluminium, A is the area of the cross-section and A_{eff} is the effective area of the cross-section considering reduced thickness owing to local buckling.

The cross-sectional resistance for bending about one principal axis (for the sections without longitudinal welds) is defined by the equation (6):

$$M_{Rd} = \alpha \cdot W_{el} \cdot f_y, \qquad \alpha = \begin{cases} W_{pl}/W_{el} & \text{for class 1} \\ W_{pl}/W_{el} & \text{for class 2} \\ 1.0 & \text{for class 3} \\ W_{eff}/W_{el} & \text{for class 4} \end{cases} \quad (6)$$

where α is the cross-sectional shape factor, W_{el} is the elastic section modulus, W_{pl} is the plastic section modulus and W_{eff} is the effective elastic section modulus considering reduced thickness owing to local buckling.

Equation (7) describes the *N-M* interaction curve of EN 1999-1 [1] for evaluating the cross-sectional resistance under combined axial compression and bending.

$$\left(\frac{N_{Ed}}{N_{Rd}}\right)^{\psi} + \left[\left(\frac{M_{y,Ed}}{M_{y,Rd}}\right)^{1.7} + \left(\frac{M_{z,Ed}}{M_{z,Rd}}\right)^{1.7}\right]^{0.6} \le 1.0, \quad \psi = \begin{cases} 1.3 & \text{for classes 1,2} \\ 1.0 & \text{for classes 3,4} \end{cases} \quad (7)$$

where N_{Ed} is the design axial compressive force, ψ is a factor depending on the cross-sectional class, $M_{y,Ed}$ and $M_{z,Ed}$ is the bending moment about the y-y and z-z axis, respectively.

The numerical results along with the European design *N-M* interaction curves for classes 1,2 and 3,4 are plotted in figure 5. For comparison purposes, the utilisation ratio of the capacity obtained in FE analysis over the predicted capacity (R_{FEA}/R_{pred}) [20] was defined for each case, as displayed in figure 6. The results are presented in Table 2 for each class separately and all together.

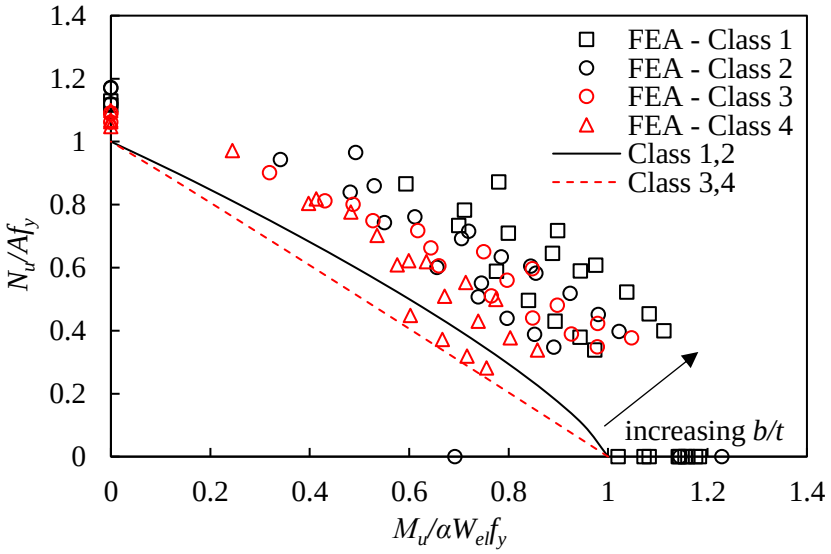

Figure 5. Assessment of European design *N-M* interaction curves for SHS/RHS aluminium alloy stub columns.

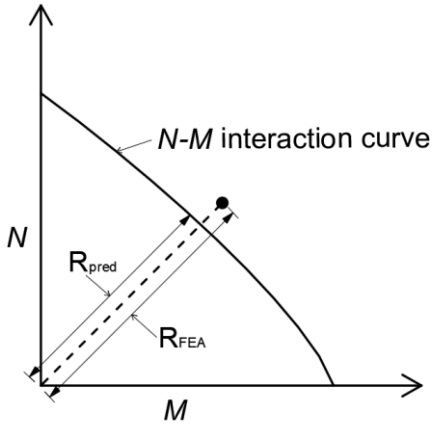

Figure 6. Definition of utilisation ratio of the FE analysis over the predicted capacity.

Table 2. Assessment of European design *N-M* interaction curves (EN 1999-1) and simplified Continuous Strength Method (CSM) according to utilisation ratio R_{FEA}/R_{pred}.

		Class				
		1	2	3	4	all
EN 1999-1	mean	1.27	1.22	1.30	1.14	**1.24**
	COV	0.11	0.11	0.08	0.08	**0.10**
simplified CSM	mean	1.16	1.14	1.17	1.30	**1.18**
	COV	0.09	0.05	0.05	0.07	**0.08**

For all cross-sectional classes the mean value of the utilisation ratio, R_{FEA}/R_{pred}, is 1.24 whereas the COV is 0.10. The fact that the mean value is higher and far from the unity indicates that EN 1999-1-1 [1] provides safe but quite conservative predictions. The same can be drawn from figure 5 where it can be observed that the FE analysis results generally exhibit the same trend with the European design *N-M* interaction curves but with an apparent scatter. Once again, the large distance between the numerical data and the Eurocode *N-M* interaction curves suggests their conservative character. Overall, EN 1999-1-1 [1] predictions for columns under eccentric axial compressive loading are safe but quite conservative which certainly is opposed to an economically efficient design process.

4. Assessment of Simplified Continuous Strength Method

The FE analysis strengths have also been utilised to evaluate the applicability of the Continuous Strength Method (CSM). CSM is a design approach allowing for the advantageous influence of material strain hardening. This approach was originally defined for stainless steel and carbon steel stocky cross-sections [21-25] and was modified so that can be applied to aluminium alloy structural elements [11]. In stocky cross-sections yielding precedes local buckling occurrence and thus, the additional strength thanks to material strain hardening could be considered during the design process. CSM was, also, extended covering the full range of cross-sectional slendernesses [26]. CSM employs a strain hardening material model which allows for strengths higher than the yield strength to be reached and a base curve to define the maximum attainable strain (ε_{CSM}). The proposed expression for the cross-sectional deformation capacity ($\varepsilon_{CSM}/\varepsilon_y$) is given by the equation (8):

$$\frac{\varepsilon_{CSM}}{\varepsilon_y} = \frac{0.25}{\bar{\lambda}_p^{3.6}} \le min(15, \frac{0.5\varepsilon_u}{\varepsilon_y}) \quad \text{for } \bar{\lambda}_p \le 0.68$$
$$\frac{\varepsilon_{CSM}}{\varepsilon_y} = \left(1 - \frac{0.222}{\bar{\lambda}_p^{1.05}}\right)\frac{1}{\bar{\lambda}_p^{1.05}} \quad \text{for } \bar{\lambda}_p > 0.68 \tag{8}$$

where ε_y is the strain at yielding and $\bar{\lambda}_p$ is the cross-sectional slenderness calculated as follows:

$$\varepsilon_y = \sqrt{f_y/E}, \qquad \bar{\lambda}_p = \sqrt{f_y/f_{cr}} \tag{9}$$

where f_y is the elastic buckling stress calculated by approximate formulae [27].
The strain hardening modulus (E_{sh}) according to the strain hardening material model may be defined from equation (10):

$$E_{sh} = \frac{f_u - f_y}{0.5\varepsilon_u - \varepsilon_y} \tag{10}$$

where f_u is the tensile strength at ultimate state and ε_u is the respective strain estimated by the equation (11):

$$\varepsilon_u = 0.13(1 - \frac{f_u}{f_y}) + 0.059 \tag{11}$$

The ultimate capacity (N_{CSM}) of a cross-section under axial compression is determined as follows:

$$\begin{aligned} N_{CSM} &= Af_{CSM} && \text{for } \bar{\lambda}_p \le 0.68 \\ N_{CSM} &= \frac{\varepsilon_{CSM}}{\varepsilon_y} Af_y && \text{for } \bar{\lambda}_p > 0.68 \end{aligned} \tag{12}$$

where f_{CSM} is calculated by the equation (13):

$$f_{CSM} = f_y + E_{sh}\varepsilon_y \left(\frac{\varepsilon_{CSM}}{\varepsilon_y} - 1 \right) \tag{13}$$

The ultimate capacity (M_{CSM}) of a cross-section under bending is taken using the following relationship:

$$\begin{aligned} M_{CSM} &= S_{pl} f_y \left[1 + \frac{E_{sh}}{E} \frac{S_{el}}{S_{pl}} \left(\frac{\varepsilon_{CSM}}{\varepsilon_y} - 1 \right) - \left(1 - \frac{S_{el}}{S_{pl}} \right) \Big/ \left(\frac{\varepsilon_{CSM}}{\varepsilon_y} \right)^2 \right] && \text{for } \bar{\lambda}_p \le 0.68 \\ M_{CSM} &= \frac{\varepsilon_{CSM}}{\varepsilon_y} S_{el} f_y && \text{for } \bar{\lambda}_p > 0.68 \end{aligned} \tag{14}$$

In this subsection, the simplified CSM [28] which suggests using the European design *N-M* interaction formulae but with CSM resistances (N_{CSM},M_{CSM}) as end points is assessed. Figure 7 displays the obtained FE results normalised by the design strengths according to CSM. The calculated utilisation ratios are, also, included in Table 2.

For all cross-sectional classes the mean value of the utilisation ratio R_{FEA}/R_{pred} is 1.18 whereas the COV is 0.08. As can be observed the simplified CSM results in slightly less conservative and scattered predictions than EN 1999-1 [1]. This can, also, be confirmed from the figure 7 where the FE results are closer to Eurocode *N-M* interaction curves demonstrating the potential of using the simplified CSM for eccentrically loaded stub columns.

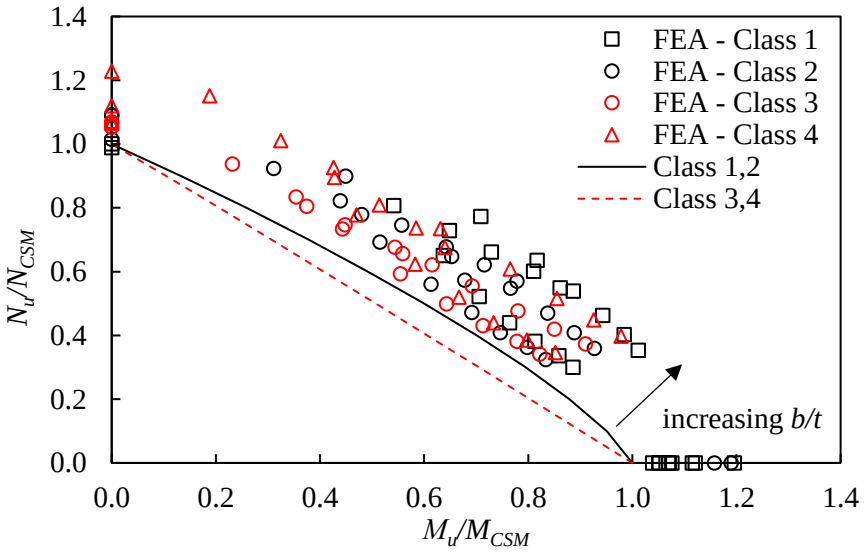

Figure 7. Assessment of simplified CSM for SHS/RHS aluminium alloy stub columns.

5. Conclusions

In the current paper a numerical study of aluminium alloy SHS/RHS stub columns subjected to eccentric axial compressive loading is presented. Material and geometric non-linearities and geometric imperfections were considered within the analyses. A parametric study was performed over a range of width-to-thickness ratios and initial loading eccentricities. The observed failure modes included material yielding, material yielding combined with inelastic local buckling and elastic local buckling. The generated data have been utilised to assess the interaction curves provided by EN 1999-1-1. The outcomes demonstrated that the predicted strengths are quite conservative particularly for the stockiest sections. The simplified CSM was, also, evaluated resulting in slightly more accurate with less scattering strength predictions.

References

[1] European Committee for Standarization (EC9) 2007 *Eurocode 9 : Design of aluminium structures. Part 1-1: General structural rules - General structural rules and rules for buildings*. BS EN 1999-1-1:2007. CEN:2007
[2] Georgantzia E, Gkantou M and Kamaris GS 2021 Aluminium alloys as structural material: A review of research *Eng. Struct.* 227. 111372
[3] Mazzolani F M, Piluso V and Rizzano G 1997 Numerical simulation of aluminum stocky hollow members under uniform compression *Proc. Int. Colloq. on Stability and Ductility of Steel Structures (Nagoya)*
[4] Langseth M and Hopperstad O S 1997 Local buckling of square thin-walled aluminum extrusions *Thin-Walled Struct.* **27**(1) 117–126
[5] Landolfo R, Piluso V, Langseth M and Hopperstad O S 1999 EC9 provisions for flat internal elements: Comparison with experimental results *Light-Weight Steel and Alum. Struct*, Mäkeläinen P and Hassinen P (The Netherlands /Elsevier) pp 515-22
[6] Faella , Mazzolani F M, Piluso V and Rizzano G 2000 Local buckling of aluminium members: Testing and classification *J. Struct. Eng.* **126**(3) 353-60
[7] Hassinen P 2000 Compression strength of aluminum columns-Experimental and numerical studies *Proc. Int. Conf. Coupled Instabilities of Metal Structures (London)* pp 241-48
[8] Mennink J 2002 *Cross-sectional stability of aluminum extrusions: Prediction of the actual local buckling behavior* Ph.D. thesis Dept. of Structural Design (Eindhoven Univ. of Technology/ Eindhoven/Netherlands)
[9] Zhu J H and Young B 2006a Tests and design of aluminum alloy compression members *J. Struct. Eng.* **132**(7) 1096-1107
[10] Zhu J H and Young B 2006b Aluminum alloy tubular columns-Part II: Parametric study and design using direct strength method *Thin-Walled Struct.* **44**(9) 969-985
[11] Su M-N, Young B and Gardner L 2014 Testing and design of aluminium alloy cross sections in compression *J. Struct. Eng.* **140**(9) 04014047
[12] Clark J W 1955 Eccentrically loaded aluminum columns *Trans. Am. Soc. Civ. Eng.* **120**(116) pp 1116-32
[13] ABAQUS. 2018 ABAQUS Standard User's Manual. Version 6.14. Providence. RI (USA): Dassault Systemes Corp.
[14] Ziemian RD 2010 *Guide to Stability Design Criteria for Metal Structures*, 6th ed. Wiley, New York, NY, USA.
[15] Zhu J H, Li Z-Q Su, M-N. and Young B. 2019 Numerical study and design of aluminium alloy section columns with welds. *Thin-Walled Struct.* **139** 139-150
[16] Wang J, Afshan S, Gkantou M, Theofanous M, Baniotopoulos C and Gardner L 2016 Flexural behaviour of hot-finished high strength steel square and rectangular hollow sections. *J Constr Steel Res* **121** 97-109

[17] Gkantou M Theofanous M Antoniou N and Baniotopoulos C 2017 Compressive behaviour of high-strength steel cross-sections. *Proc. of the Inst. of Civil Engineers-Structures and Buildings* **170**(11) 813-824
[18] Georgantzia E, Bin Ali S, Gkantou M, Kamaris G S, Kansara K and Atherton W 2021 Structural response of aluminium alloy concrete filled tubular columns. *Proc. of Eurosteel (Sheffield)*
[19] Hill HN. 1944 Determination of stress-strain relations from "offset" yield strength values Technical Note No. 927
[20] Gkantou M, Theofanous M, Wang J, Baniotopoulos C and Gardner L 2017 Behaviour and design of high strength steel cross-sections under combined loading. *Proc. of the Inst. of Civil Engineers-Structures and Buildings*
[21] Gardner L and Ashraf M 2006 Structural design for non-linear metallic materials *Eng. Struct.* **28**(6) 926–934
[22] Gardner L 2008 The continuous strength method *Proc. Inst. Civ.Eng.: Struct. Build.* **161**(3) pp 127–133
[23] Gardner L and Theofanous M 2008 Discrete and continuous treatment of local buckling in stainless steel elements *J. Constr. Steel Res.* **64**(11) 1207-16
[24] Gardner L, Wang F and Liew A 2011 Influence of strain hardening on the behavior and design of steel structures *Int. J. Struct. Stab. Dyn.* **11**(5) pp 855-75
[25] Afshan S and Gardner L 2013 The continuous strength method for structural stainless steel design *Thin-Walled Struct.* **68** 42-9
[26] Su M-N Young B and Gardner L 2016 The continuous strength method for the design of aluminium alloy structural elements. *Eng. Struct.* **122** 338-348
[27] Seif M and Schafer BM 2010 Local buckling of structural steel shapes *J Constr Steel Res* **66**(10) 1232-47
[28] Zhao O, Rossi B, Gardner L and Young B 2015 Behaviour of structural stainless steel cross-sections under combined loading. I: Numerical modelling and design approach *Eng. Struct.* **89** 247-259